

Statistical model applied to $A_xB_yC_{1-x-y}D$ quaternary alloys: Bond lengths and energy gaps of $Al_xGa_yIn_{1-x-y}X$ ($X=As, P, \text{ or } N$) systems

M. Marques,¹ L. K. Teles,² L. G. Ferreira,³ L. M. R. Scolfaro,¹ J. Furthmüller,⁴ and F. Bechstedt⁴

¹*Instituto de Física, Universidade de São Paulo CP66318, 05315-970 São Paulo, SP, Brazil*

²*Departamento de Física, Instituto Tecnológico de Aeronáutica, Centro Técnico Aeroespacial, 12228-900 São José dos Campos, SP, Brazil*

³*Instituto de Física Gleb Wataghin, Universidade Estadual de Campinas, Caixa Postal 6165, 13083-970 Campinas, SP, Brazil*

⁴*Institut für Festkörperteorie und Theoretische Optik, Friedrich-Schiller-Universität, 07743 Jena, Germany*

(Received 16 December 2005; revised manuscript received 23 February 2006; published 14 June 2006)

We extend the generalized quasichemical approach (GQCA) to describe the $A_xB_yC_{1-x-y}D$ quaternary alloys in the zinc-blende structure. Combining this model with *ab initio* ultrasoft pseudopotential calculations within density functional theory, the structural and electronic properties of $Al_xGa_yIn_{1-x-y}X$ ($X=As, P, \text{ or } N$) quaternary alloys are obtained, taking into account the disorder and composition effects. Results for the bond lengths show that the variation with the compositions is approximately linear and also does not deviate very much from the value of the corresponding binary compounds. The maximum variation observed amounts to 3.6% for the In-N bond length. For the variation of band gap, we obtain a bowing parameter $b=0.26$ eV for the $(Ga_{0.47}In_{0.53}As)_z(Al_{0.48}In_{0.52}As)_{1-z}$ quaternary alloy lattice matched to InP, in very good agreement with experimental data. In the case of AlGaInN, we compare our results for the band gap to data for the wurtzite phase. We also obtained a good agreement despite all evidences for cluster formation in this alloy. Finally, a bowing parameter of 0.22 eV is obtained for zinc-blende AlGaInN lattice matched with GaN.

DOI: [10.1103/PhysRevB.73.235205](https://doi.org/10.1103/PhysRevB.73.235205)

PACS number(s): 61.66.Dk, 64.75.+g, 71.20.Nr

I. INTRODUCTION

The need to simultaneously control both the band gap and the lattice constant of semiconductor alloys prompted interest not only in ternary but also quaternary alloys of the kind $A_xB_yC_{1-x-y}D$. The composition variations allow an independent variation of the lattice constant and of the energy gap of the alloy, and, hence, the production of lattice-matched heterostructures, with a low defect density. In this sense, systems such as the quaternary $(Al_{0.48}In_{0.52}As)_z(Ga_{0.47}In_{0.53}As)_{1-z}$ alloy lattice matched to InP, and $(Al_xGa_{1-x})_{0.50}In_{0.50}P$ lattice matched to GaAs, are already widely studied experimentally. Recently, the nitride-based quaternary $Al_xGa_yIn_{1-x-y}N$ alloy became a largely employed material among the nitrides due to the possibility lattice matched grown on GaN. Besides, it has been also observed that the incorporation of indium in the ternary AlGaIn alloy improves significantly the ultraviolet (UV) emission. All mentioned systems have been widely used in electronic and optoelectronic device technology. Important device examples are the recently reported efficient UV light emitting diodes and laser diodes comprising quaternary AlGaInN/AlGaInN multiple quantum wells,¹⁻⁴ the current generation of digital video disks, which uses an AlGaInP red laser with an emission wavelength of 650 nm, and the $Al_xGa_yIn_{1-x-y}As/InP$ lattice matched system used for device applications relevant to optical communications, such as emitters, wave guides, lasers, and infrared detectors.^{5,6}

A striking property of the AlGaInN alloys that influences remarkably the emission processes is the tendency for phase separation.⁷⁻¹¹ More recently,^{12,13} first-principles calculations followed by Monte Carlo simulations of the thermodynamic properties of the $(Al, Ga, In)X$ ($X=As, P, \text{ or } N$) systems showed that the arsenides and phosphides are very stable

against phase separation while the quaternary nitrides on the contrary are thermodynamically unstable. In the latter case, the instability leads to the formation of In-rich clusters or InGaIn-like nanoclusters depending on the In and/or Al concentrations. The large differences in the equilibrium lattice constants of the binary compounds result in a considerable internal strain. It drives the tendency of phase separation in the alloy. For the structural properties of $(Al, Ga, In)X$ ($X=As, P, \text{ or } N$) there is no theoretical work reported thus far that contemplates a reasonably sized model supercell and the statistics of the alloy. Moreover, another open question is the composition dependence of the energy gap of the random alloys in order to analyze the emission processes.

In this work, we develop a rigorous theoretical model to study the structural and electronic properties of $Al_xGa_yIn_{1-x-y}X$ ($X=As, P, \text{ or } N$) quaternary alloys. The first-principles calculations performed here are based on an *ab initio* ultrasoft pseudopotential method within the framework of density functional theory and the local density approximation, which is implemented in the “Vienna *ab initio* simulation package” (VASP). The thermodynamic calculations are based on a generalization of the quasichemical approach combined with a cluster expansion of the thermodynamic potentials. As recently reported by us for the AlGaIn, InGaIn, InAlIn, BGaN, and BAlN ternary alloys,¹⁴⁻¹⁸ the cluster expansion is able to successfully describe the physical properties of group-III nitride alloys. Here the cluster treatment is generalized to study quaternary (pseudoternary) alloys. We focus our attention mainly on the cubic (c-) $Al_xGa_yIn_{1-x-y}X$ ($X=As, P, \text{ or } N$) alloys, and present results for the bond lengths and the energy band gaps as functions of the alloy compositions x and y . For the comparison to experimental band gap data, we concentrate our analysis on the important specific compositions in which AlGaInN, AlGaInP, and

AlGaInAs are lattice matched, respectively, to GaN, GaAs, and InP substrates.

The paper is organized as follows. In Sec. II, we describe the theoretical methods adopted for the calculations, while the results and a detailed discussion of the alloy behavior and properties are given in Sec. III. Finally, Sec. IV is devoted to the conclusions.

II. THEORETICAL MODEL

The standard generalized quasi-chemical approximation (GQCA) within the framework of the cluster expansion method has been successfully applied to describe binary and ternary semiconductor alloys.^{14–18} Here we extend the method to the $A_xB_yC_{1-x-y}D$ quaternaries. The alloy atoms A, B, and C, the cations, should occupy one fcc sublattice while the D atoms, the anions, occupy the other one. In the cation sublattice, we consider K sites on which A, B, and C atoms assume some configurations. The average numbers of A, B and C atoms are

$$\begin{aligned} K_A &= xK, \\ K_B &= yK, \\ K_C &= (1-x-y)K, \\ K &= K_A + K_B + K_C. \end{aligned} \quad (1)$$

The alloy is divided into an ensemble of individual clusters statistically and energetically independent of the surrounding atomic configuration. We first decompose the system into M clusters of $2n$ -atoms ($K=nM$) each. We classify the various species of clusters into $(J+1)$ groups of distinct cluster energies ε_j with $j=0, 1, 2, \dots, J$. For a particular configuration, there are M_j clusters of energy ε_j . Each cluster j with a certain number of A, B, and C atoms is realized with a certain probability $x_j=M_j/M$, such that

$$\sum_{j=0}^J x_j = 1. \quad (2)$$

Aside from the energy, the clusters can also differ with respect to the number n_j of A atoms, m_j of B atoms, and $(n-n_j-m_j)$ of C atoms. These numbers underlie two constraints due to the given averaged compositions x and y

$$\begin{cases} \sum_{j=0}^J n_j x_j = nx \\ \sum_{j=0}^J m_j x_j = ny \end{cases}. \quad (3)$$

According to the Connolly-Williams method,¹⁹ the constraints (3) can be interpreted as a special case of the representation of the configurationally averaged and, hence, composition-dependent (and, in general, also temperature-dependent) value

$$P(x, y, T) = \sum_{j=0}^J x_j(x, y, T) P_j \quad (4)$$

of a property P of interest of the quaternary alloy with mainly compositional disorder. Of course, the considered property is different for each cluster and depends on the cluster class index j according to P_j .

The definition above allows the introduction of fluctuations around the mean values by considering the root-mean-square (rms) deviations

$$\Delta P(x, y, T) = \left[\sum_{j=0}^J x_j(x, y, T) P_j^2 - \left(\sum_{j=0}^J x_j(x, y, T) P_j \right)^2 \right]^{1/2}. \quad (5)$$

Then the total energy (more strictly the internal energy) of the alloy at a fixed temperature T can be described by the relation

$$U(x, y, T) = M \sum_{j=0}^J x_j(x, y, T) \varepsilon_j. \quad (6)$$

The mixing free energy ΔF is defined by

$$\Delta F(x, y, T) = F(x, y, T) - xF_{AD} - yF_{BD} - (1-x-y)F_{CD}, \quad (7)$$

where F , F_{AD} , F_{BD} , and F_{CD} are, respectively, the Helmholtz free energies for the alloy and for the pure AD, BD, and CD compounds containing the same number of D atoms. Thus, ΔF can be written as

$$\Delta F(x, y, T) = \Delta U(x, y, T) - T\Delta S(x, y, T), \quad (8)$$

where ΔU is the mixing alloy enthalpy defined as

$$\begin{aligned} \Delta U(x, y, T) &= M \sum_{j=0}^J x_j(x, y, T) \varepsilon_j - M[x\varepsilon_{AD} + y\varepsilon_{BD} \\ &\quad + (1-x-y)\varepsilon_{CD}]. \end{aligned} \quad (9)$$

The configurational or mixing entropy can be calculated from Boltzmann's definition $\Delta S = k_B \ln W$, where W is the number of ways to configure the alloy with the set M_0, M_1, \dots, M_J of clusters. This number of configurations W is given by a product of three quantities. First, the total number of ways $K!/(K_A!K_B!K_C!)$, in which K_A A atoms, K_B B atoms, and K_C C atoms can be placed on K sites. Second, this number has to be multiplied by $M!/(\prod_{j=0}^J M_j!)$, that is the number of ways to arrange the different clusters M_0, M_1, \dots, M_J . Third, with the assumption that the various clusters are independent, one has to multiply by the joint probability of finding the set of clusters M_0, M_1, \dots, M_J in the alloy, $\prod_{j=0}^J (x_j^0)^{M_j}$, with

$$x_j^0 = g_j x^{n_j} y^{m_j} (1-x-y)^{n-n_j-m_j} \quad (10)$$

being the fraction of clusters of type j for a given composition x of A and y of B as obtained within a regular solid solution model.²⁰ The degeneracy factor g_j is the number of ways to arrange the alloying cations in a cluster with energy ε_j and depends on the size and symmetry of the cluster. In

this work, 16 atom supercells are used as the basic clusters, with eight cations and eight anions. For example, in the case with one A atom, three B atoms, and four C atoms, there are a total of 248 ways to arrange these atoms in the eight cation positions of the supercell. But there are only five kinds of clusters that are inequivalent by symmetry, with the degeneracy factors g_j 32, 32, 96, 96, and 24. Summarizing, one has

$$W = \frac{K!}{K_A!K_B!K_C!} \frac{M!}{\prod_{j=0}^J M_j!} \prod_{j=0}^J (x_j^0)^{M_j}. \quad (11)$$

In the Stirling limit, it follows for the mixing entropy that

$$\Delta S(x, y, T) = -k_B \left\{ K[x \ln x + y \ln y + (1-x-y)\ln(1-x-y)] + M \sum_{j=0}^J x_j \ln \left(\frac{x_j}{x_j^0} \right) \right\}. \quad (12)$$

The cluster fractions x_j are unknown. A simple approach to the numerical problem is to use the Lagrange multipliers formalism in the constraints (2) and (3) of a variational calculation for the x_j , i.e.,

$$\frac{\partial}{\partial x_j} \left[\frac{\Delta F(x, y, T)}{M} - \lambda_1 \left(\sum_{i=0}^J x_i - 1 \right) - \lambda_2 \left(\sum_{i=0}^J x_i n_i - nx \right) - \lambda_3 \left(\sum_{i=0}^J x_i m_i - ny \right) \right] = 0, \quad (13)$$

where λ_1, λ_2 , and λ_3 are Lagrange multipliers. With the definitions $\eta_x = \frac{x e^{\lambda_2 \beta}}{(1-x-y)}$, $\eta_y = \frac{y e^{\lambda_3 \beta}}{(1-x-y)}$, and $\beta = 1/k_B T$, we find for the statistical weights

$$x_j(x, y, T) = \frac{g_j \eta_x^{n_j} \eta_y^{m_j} e^{-\beta \varepsilon_j}}{\sum_{i=0}^J g_i \eta_x^{n_i} \eta_y^{m_i} e^{-\beta \varepsilon_i}}. \quad (14)$$

The unknown parameters η_x and η_y are determined from the condition that the expression (14) fulfills the constraints (3), leading to the coupled polynomial equations

$$\begin{cases} \sum_{j=0}^J g_j \eta_x^{n_j} \eta_y^{m_j} e^{-\beta \varepsilon_j} (xn - n_j) = 0 \\ \sum_{j=0}^J g_j \eta_x^{n_j} \eta_y^{m_j} e^{-\beta \varepsilon_j} (yn - m_j) = 0 \end{cases}. \quad (15)$$

Among all possible solutions of the above coupled equations, only the positive root has a meaning in the theory and we verified that this solution is unique.

The total energy of each cluster is calculated by adopting a first-principles pseudopotential plane-wave VASP code²¹ based on the density functional theory (DFT) in the local density approximation (LDA).²² Besides the valence electrons also the semicore Ga3d and In4d states are explicitly considered. Their interaction with the atomic cores is treated by non-norm-conserving *ab initio* Vanderbilt

pseudopotentials.²³ We assumed an energy cutoff of 331.5 eV for AlGaInN quaternary alloy calculation and 313.4 eV for AlGaInP and AlGaInAs. The many-body electron-electron interaction is described within the Ceperley-Alder scheme as parametrized by Perdew and Zunger.²⁴ The \mathbf{k} -space integrals are approximated by sums over a $4 \times 4 \times 4$ special-points of the Monkhorst-Pack type²⁵ within the irreducible part of the Brillouin zone. As the basic clusters to describe the fully relaxed alloys, we use supercells, that form hexahedrons (stretched cubes along a body diagonal), which have 16 atoms (8 cation sites).¹³ Considering the symmetry, there are 141 kinds $j=0, \dots, 140$ ($J=140$) of clusters distinguished by distinct cluster energies ε_j . The total energy calculations of the 141 cluster configurations are performed at $T=0$ K (the temperature dependence is taken into account in the statistics as described above). All atomic coordinates in the supercell are relaxed until the Hellmann-Feynman forces vanish, using as the criterion that the energy difference between two successive changes of atomic positions is $\leq 10^{-4}$ eV. For the nitride alloy, the structure of each cluster is optimized with respect to its lattice constant, via total energy minimization, while for the arsenides and phosphides we assume the validity of Vegard's law.

III. RESULTS AND DISCUSSION

A. Bond lengths

We begin with the application of the GQCA method to obtain the first-neighbor distances, i.e., the bond lengths Al-X, Ga-X, and In-X ($X=N, P, \text{ or } As$) in the $Al_xGa_yIn_{1-x-y}X$ alloys with varying Al, Ga, and In compositions. We verified that the influence of the temperature variation, in the range of typical growth temperatures of these quaternary alloys, is completely negligible in the evaluation of the probabilities x_j entering expressions (4) and (5). Therefore, we use the temperature of 1000 K in all cases. The definition of the configurational average of a quantity has to be generalized for the first-neighbor distances d_{A-D} , since different types of atomic pairs A-D exist in one cluster. It is now

$$d_{A-D}(x, y) = \frac{\sum_{j=0}^J x_j(x, y) k_j^{A-D} d_j^{A-D}}{\sum_{j=0}^J x_j(x, y) k_j^{A-D}}, \quad (16)$$

where k_j^{A-D} is the fraction of A-D bond lengths in the cluster and d_j^{A-D} is the average bond length between the cation A and anion D. There is the constraint $k_j^{A-D} + k_j^{B-D} + k_j^{C-D} = 1$ for each cluster type j . The characteristic bond lengths d_j^{A-D} are taken for each cluster from the results of the total-energy optimization.

We first present the results obtained for the structural properties of the $Al_xGa_yIn_{1-x-y}N$ alloy, i.e., for the configurationally averaged bond lengths $d_{Al-N}(x, y)$, $d_{Ga-N}(x, y)$, and $d_{In-N}(x, y)$, as functions of the alloy contents, x and y . For the

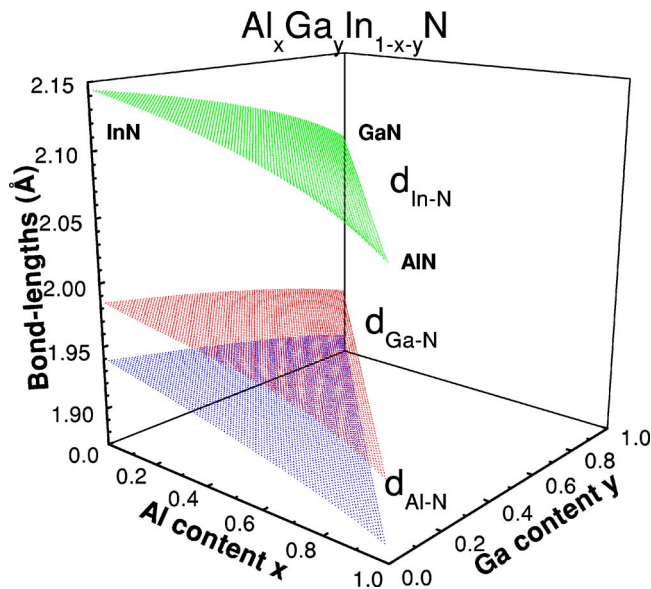


FIG. 1. (Color online) Al-N, Ga-N, and In-N bond lengths ($d_{\text{Al-N}}$, $d_{\text{Ga-N}}$, and $d_{\text{In-N}}$, respectively) as functions of the Al content x and Ga content y for $\text{Al}_x\text{Ga}_y\text{In}_{1-x-y}\text{N}$ alloys.

nitrides, all 141 cluster have an optimized lattice constant.²⁶ The values obtained for the binaries compounds are $a_{\text{AlN}}=4.34 \text{ \AA}$, $a_{\text{GaN}}=4.46 \text{ \AA}$, and $a_{\text{InN}}=4.95 \text{ \AA}$. The results are depicted in Fig. 1. Three curved surfaces (which are *almost planelike* and parallel) of bond lengths $d_{\text{Al-N}}$, $d_{\text{Ga-N}}$, and $d_{\text{In-N}}$ in the x - y plane can be observed. This indicates that, independent of the composition, the alloy system tends to have bond lengths with the same values as in the corresponding binary compounds. However, analyzing the Fig. 1 in more detail, we see that the bond lengths are not completely composition independent. With increasing x and y values, the lattice parameter decreases and, consequently, also do the bond lengths. As in the case of the binary compounds, the distance $d_{\text{In-N}}$ is the largest one among the three bond lengths $d_{\text{Al-N}}$, $d_{\text{Ga-N}}$, and $d_{\text{In-N}}$. The maximum variation for each bond length is 0.058, 0.059, and 0.078 \AA for the $d_{\text{Al-N}}$, $d_{\text{Ga-N}}$, and $d_{\text{In-N}}$, respectively. In the case of $d_{\text{In-N}}$, it only deviates by 3.6% from the value at the binary InN. In Table I, we fit linear expressions for the bond lengths as functions of the compositions x and y to the results of expressions of the type (16). As can be verified from the maximum errors (percentage difference between the fitted and the calculated value) in the third column, the fitting expression is rather satisfactory (0.55% error for the worst case). The same linear (planar)

TABLE I. Bond length as a linear function of the compositions x and y for the $\text{Al}_x\text{Ga}_y\text{In}_{1-x-y}\text{N}$ quaternary alloy. The deviation from the fit errors are also presented.

Bond length	Fit function	Maximum error (%)
Al-N	$1.9435 - 0.05090x - 0.05455y$	0.19
Ga-N	$1.9919 - 0.05985x - 0.06050y$	0.35
In-N	$2.1573 - 0.08292x - 0.07570y$	0.55

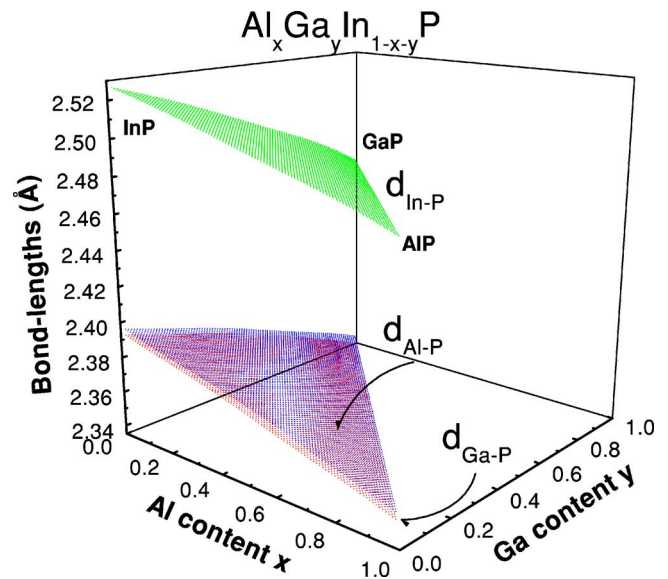


FIG. 2. (Color online) Al-P, Ga-P, and In-P bond lengths ($d_{\text{Al-P}}$, $d_{\text{Ga-P}}$, and $d_{\text{In-P}}$, respectively) as functions of the Al content x and Ga content y for $\text{Al}_x\text{Ga}_y\text{In}_{1-x-y}\text{P}$ alloys.

behavior was similarly observed for the ternary alloys.^{14,15,27-29} Moreover, we verify that only the average bond length corresponding weighted concentrations follows Vegard's law, i.e., varying linearly between the bond lengths of the binary compounds. This result is in agreement with the behavior of the lattice constant of the mixed crystal.²⁶

For the arsenides and phosphides, we only minimize the binary compounds and assume that Vegard's law is fulfilled. For the binaries, we found for the lattice constants $a_{\text{AlAs}}=5.63 \text{ \AA}$, $a_{\text{GaAs}}=5.61 \text{ \AA}$, $a_{\text{InAs}}=6.04 \text{ \AA}$, $a_{\text{AlP}}=5.43 \text{ \AA}$, $a_{\text{GaP}}=5.39 \text{ \AA}$, and $a_{\text{InP}}=5.84 \text{ \AA}$. These values differ <1% from the experimental ones.³⁰ In Fig. 2 and 3, we show the results for the bond lengths of the phosphides and arsenides alloys,

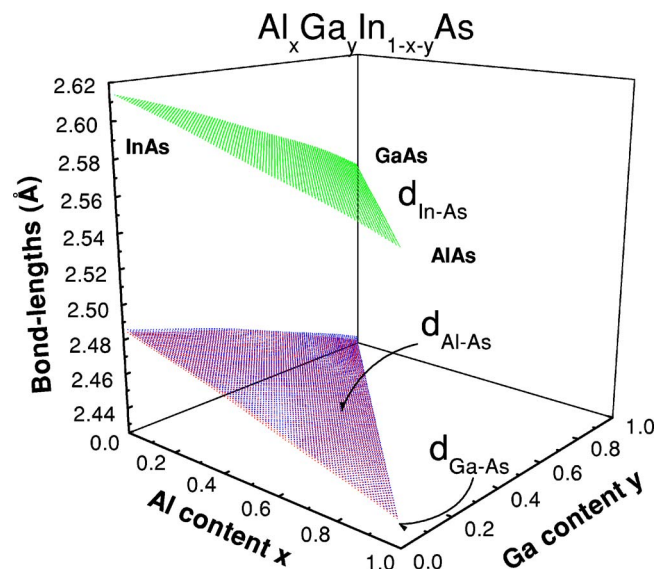


FIG. 3. (Color online) Al-As, Ga-As, and In-As bond lengths ($d_{\text{Al-As}}$, $d_{\text{Ga-As}}$, and $d_{\text{In-As}}$, respectively) as functions of the Al content x and Ga content y for $\text{Al}_x\text{Ga}_y\text{In}_{1-x-y}\text{As}$ alloys.

TABLE II. Bond length as a linear function of the compositions x and y for the $Al_xGa_yIn_{1-x-y}P$ and $Al_xGa_yIn_{1-x-y}As$ quaternary alloys. The deviation from the fit errors are also presented.

Bond length	Fit function	Maximum error (%)
Al-P	$2.3992 - 0.04685x - 0.05787y$	0.10
Ga-P	$2.3962 - 0.04843x - 0.05915y$	0.10
In-P	$2.5311 - 0.04996x - 0.06746y$	0.14
Al-As	$2.4888 - 0.04978x - 0.05791y$	0.08
Ga-As	$2.4875 - 0.05022x - 0.05859y$	0.09
In-As	$2.6180 - 0.05140x - 0.06676y$	0.12

respectively. We observe that, in these cases, the maximum variation of the bond lengths is 0.065 \AA , which means a lesser composition dependence in comparison to the nitrides. At the same time, we observe a more linear behavior, which is confirmed by the smaller values of the maximum deviation between the calculated and fitted values, as shown in Table II. Moreover, the bond lengths d_{Al-X} and d_{Ga-X} ($X=As$ or P) are similar. We observe a smaller spacing between the planes, resulting in a smaller internal strain, which can be a major factor to explain why the ternary arsenides and phosphides are more stable than the nitrides. The results for the lattice parameters and bond lengths of nitrides, phosphides and arsenides are not surprising. N, being a much smaller atom than P and As, gives rises to smaller interatomic distances; thus, in the nitrides, the distances are remarkably determined by the cations being alloyed. In the phosphides and arsenides, on the other hand, the contributions of the cations is relatively smaller. As far as we know, there are no experimental data available for these quaternary alloys. Therefore, we compare our results to other theoretical results by Chen and Fan³¹ for AlGaInAs. They used a tight-binding theory combined with the virtual crystal approximation to describe the alloy. Our result indicates a maximum distortion of 2.4% for In-As bond length compared to 1.8% predicted by that work.

B. Band gaps

Now we present the results for the electronic properties for the quaternary alloys, more precisely the dependence of the fundamental band gap on the Al (x) and Ga (y) contents. Although we study systems with chemical disorder, which do not possess a band structure resulting from a translational symmetry, it is still possible to define, both theoretically and experimentally, band gap energies. Before we obtain the energy gap for each cluster, we have to consider that our 16 atom supercells present a smaller Brillouin zone than the unitary cell of the zinc blende structure. Thereby, the points of high symmetry Γ , X , L , and K are folded onto the Γ point in the little Brillouin zone. Nevertheless, for the nitrides, it is possible to separate the direct Γ - Γ band gap from the indirect Γ - X band gap, despite the fact that the band gap for each cluster used is the direct band gap. However, in the case of arsenides and phosphides, at least for some clusters, the con-

duction band states at R and K are between Γ and X . This does not allow us to identify of the states and distinguish between the direct Γ - Γ band gap and Γ - X band gap. In these latter cases, as the band gap of each cluster we simply use the difference between the highest occupied state and the lowest empty state at the $k=(0,0,0)$ point. Another issue to consider is the well-known underestimation of the band gap obtained within DFT-LDA calculations. In order to correct the DFT-LDA results, the calculated values for E_g have been shifted by a linear function of two variables. Fortunately, the quasiparticle corrections vary almost linearly with the composition as shown previously for the ternary nitride alloys.³² Therefore, the bowing parameter obtained by the GQCA-DFT is reliable and can be compared to experimental data. We assume the same behavior for the quaternary alloys. Thus, in order to correct the DFT-LDA results, the calculated values for E_g have been shifted by a plane surface.

First, we present the results for the $Al_xGa_yIn_{1-x-y}N$ quaternary alloy. Until now, there are only preliminary results in cubic samples of AlGaInN quaternary alloys quoted in the literature.³³ Therefore, we compare the composition dependence of the band gap to experimental data obtained for wurtzite alloys. Although we use the cubic (zinc-blende) structure for the calculations, the results for the composition dependence may be expected to apply equally for the wurtzite counterpart due to their equal nearest-neighbors structure. Thus, we assume that the bowing parameters for the quaternary AlGaInN alloys are the same in the wurtzite and the zinc-blende mixed crystals. A plane shift of the energy gap preserves the two-dimensional bowing in the x - y plane. Therefore, the plane surface is defined by adding corrections in order to obtain the experimental values for the energy band gaps of the binary compounds AlN, GaN and InN, i.e.,

$$E_g(x,y) = E_g^{\text{GQCA-LDA}}(x,y) + x\Delta E_g^{\text{AlN}} + y\Delta E_g^{\text{GaN}} + (1-x-y)\Delta E_g^{\text{InN}}, \quad (17)$$

with $E_g^{\text{GQCA-LDA}}$ being the energy gap of the quaternary alloy, as obtained from a GQCA-DFT-LDA calculation, and ΔE_g^{AN} ($A=Al, Ga, \text{ or } In$) the quasiparticle correction parameters in order to obtain the experimental band gap for the wurtzite phase of the binary compounds AlN ($x \rightarrow 1$), GaN ($y \rightarrow 1$) and InN [$(1-x-y) \rightarrow 1$]. We apply the following experimental values for the *direct* band gaps of the nitrides in the wurtzite phase: $E_g^{\text{exp}}(\text{AlN})=6.2 \text{ eV}$, $E_g^{\text{exp}}(\text{GaN})=3.4 \text{ eV}$, and $E_g^{\text{exp}}(\text{InN})=0.7 \text{ eV}$.³⁴⁻³⁷ We emphasize here that we have already published²⁶ a complete expression for the band gap as a function of the contents x and y , together with a band-gap surface. The values for the direct energy band gap obtained, $E_g^{\Gamma-\Gamma}(x,y)$, may be confronted with the experimental values that are available in the literature for the w -phase materials. A survey of experimental data as extracted from photoluminescence (PL) measurements performed on different $Al_xGa_yIn_{1-x-y}N$ alloy samples is shown in Table III. The table compares experimental data to the results obtained within our model, where we suppose an emission caused by a band-to-band transition in a matrix of AlGaInN, where the Al, Ga, and In atoms are randomly distributed over one sublattice. Excitonic effects are omitted from the discussion.

TABLE III. Comparison between the calculated ($E_g^{\text{calc.}}$) and the experimental ($E_g^{\text{exp.}}$) values of the energy gap of several samples of AlGaInN quaternary alloys grown on GaN. The first column presents the In and Al contents of the samples.

$(1-x-y;x)$	Ref.	$E_g^{\text{exp.}}$ (eV)	$E_g^{\text{calc.}}$ (eV)
(0.03;0.10)	39	3.41	3.51
(0.02;0.10)	40	3.65	3.55
(0.04;0.14)	48	3.47	3.56
(0.026;0.124)	1	3.58	3.58
(0.10;0.03)	49	2.98	3.04
(0.026;0.124)	11	3.58	3.58
(0.02;0.15)	10	3.70	3.68
(0.02;0.15)	10	2.37	3.68
(0.18;0.21)	41	2.38	3.18
(0.38;0.60)	41	2.38	3.40

Except for the last three rows in Table III, one observes a very good agreement between theoretically predicted values and the experimental ones. In principle, one can state that, despite the approximations made, our model describes very well the variation of the band gap with the contents of Al and Ga atoms in the quaternary nitrides alloys. However, there are other points to be considered. The assumption of a stable random alloy is not so reliable for nitride mixed crystals. There is evidence from measurements¹¹ that the strong emission observed in such alloys is caused by a more efficient emission mechanism than the band-to-band transition, e.g., that originated from confined states in GaInN clusters. In addition to that, previous theoretical work^{12,13} presented a complete microscopic description of the phase separation process in AlGaInN quaternary alloys. There has been shown the formation of the GaInN clusters in agreement with this experimental result. In this context, the good agreement of the calculated composition dependence with experimental data can comprises two different situations: (i) The UV emission comes from the AlGaInN matrix and our model predicts efficiently the band gap of the AlGaInN quaternary alloy; and (ii) the UV emission is originated in the GaInN clusters, and the good spectral agreement is a coincidence due to the relatively small x values studied in Table III. The work of Chen *et al.*¹¹ showed that the spectral shift between the efficient GaInN cluster emission and the inefficient AlGaInN matrix UV emission is about 100 meV in the studied sample. This value corresponds to our largest difference between experimental^{39,40} and calculated gap values in Table III. The last three rows in Table III, which show large deviations from experiment, indicate emission in the green spectral range, which should be due to InN-rich phases,^{10,41} as suggested previously.^{12,13}

As a further interesting electronic property of the AlGaInN alloys, we present the energy gap variation with composition for the important specific case that the alloy lattice is matched with a GaN substrate. This happens for $y = 1.00 - 1.23x$.²⁶ Results are presented in Fig. 4. The energy gap correction was not made because there is no reliable data

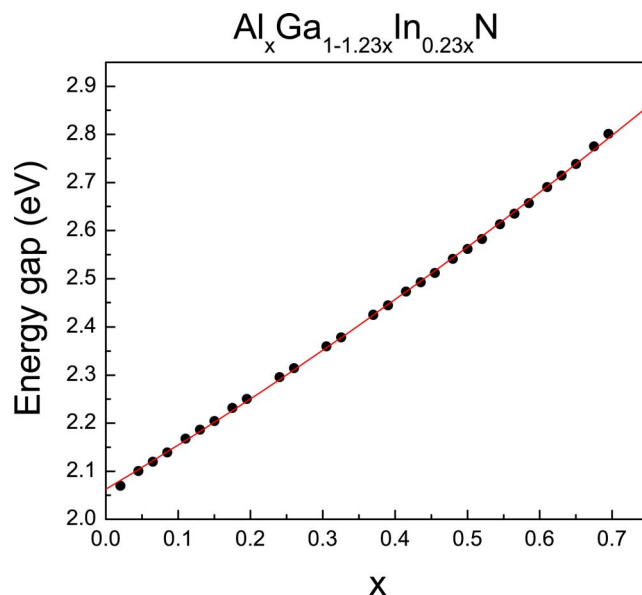


FIG. 4. (Color online) Energy gap as function of Al content x for $\text{Al}_x\text{Ga}_{1-1.23x}\text{In}_{0.23x}\text{N}$ alloys been lattice matched with GaN. The circles are the results of the calculation, and the solid line represents a fit.

for zinc-blende InN and AlN direct energy gaps in the literature. We fit a simple quadratic expression to the calculated GQCA-LDA values and obtain a bowing parameter of $b = 0.22$ eV, for the variation of energy gap as function of Al content x . As results for band gap of zinc-blende AlGaInN samples do not exist in the literature, this value can be considered as a prediction of the bowing parameter in these systems, and also, as shown by our comparison to wurtzite data, a good approximation for the bowing parameter for the wurtzite AlGaInN lattice matched with GaN.

For the $\text{Al}_x\text{Ga}_y\text{In}_{1-x-y}\text{As}$ quaternary alloys the problem of phase separation¹³ does not exist and this alloy can be considered as presenting a truly random distribution of atoms. Therefore, the GQCA model can be applied without restrictions to describe the alloy. We present the band-gap behavior in the range of compositions for which the alloy is lattice matched to InP, that is $(\text{Ga}_{0.47}\text{In}_{0.53}\text{As})_z(\text{Al}_{0.48}\text{In}_{0.52}\text{As})_{1-z}$, with z varying from 0 to 1. Such an alloy may be thought of as a combination of two arsenide ternary alloys. The gap variation is shown in Fig. 5. The curve obtained with GQCA-LDA was corrected to account for the DFT-LDA gap underestimation. In order to obtain band gaps comparable to experiment, we add the composition-dependent quasiparticle $[0.8269 + 0.0784x]$ eV. In this case, the limits, the ternary alloys, have band gaps equal to the experimental ones, 0.75 eV for the $\text{Ga}_{0.47}\text{In}_{0.53}\text{As}$ alloy and 1.47 eV for the $\text{Al}_{0.48}\text{In}_{0.52}\text{As}$ alloy.⁴² A quadratic fit leads to the bowing parameter, which indicates how much the behavior of band gap as a function of composition deviates from linearity. We obtain the following expressions, written as a function of Al content x or the more convenient, for this specific case, as function of the parameter z ,

$$E_g(x) = [0.75 + 0.964x + 1.117x^2] \text{ eV},$$

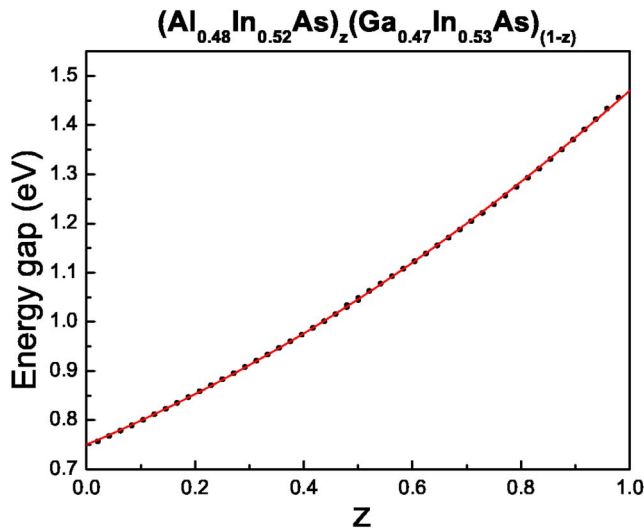


FIG. 5. (Color online) Energy gap as function z for $(\text{Ga}_{0.47}\text{In}_{0.53}\text{As})_z(\text{Al}_{0.48}\text{In}_{0.52}\text{As})_{1-z}$ alloys, with z varying from 0 to 1. These alloys are lattice matched with InP. The circles are the results of the calculation, and the solid line corresponds to the fit.

$$E_g(z) = [0.75 + 0.463z + 0.257z^2] \text{ eV}. \quad (18)$$

The quadratic fit to the calculated gaps (full circles) is excellent, i.e., a constant bowing describes the behavior of the band gap as function of mixing z . In order to compare our result to the literature, we discuss the standard bowing coefficient for the alloy dependence on z . An initial characterization of this quaternary alloy was made by Olego *et al.*⁶ They obtained a bowing parameter of 0.20 eV.⁶ Subsequent measurements of photoluminescence (PL) of Kopf *et al.*⁴³ and Cury *et al.*⁴⁴ showed a linear variation of the band gap ($b=0$). However, Böhler *et al.*,⁴⁵ with low-temperature PL measurements, obtained a large bowing value of $b=0.68$ eV. Fan and Chen⁴⁶ obtained a value of $b=0.225$ eV for the full range of x and z , for samples lattice matched to InP. Our bowing parameter, $b=0.257$ eV, is in excellent agreement with the results of Olego *et al.*⁶ and Fan and Chen.⁴⁶ Based on these results, the review paper of Vurgaftman *et al.*⁴⁷ suggests an average value of 0.22 eV for b , which is therefore also in excellent agreement with our re-

sult. We also compare our result to a previous calculation of Chen and Fan³¹ This *tight-binding* calculation uses the virtual crystal approximation in order to simulate the alloy and is an approach less rigorous than the approach that we developed here. The authors obtained no bowing ($b=0$) for this alloy, a result that disagrees with the majority of parameters discussed above. The AlGaInP quaternary alloy is lattice matched to GaAs for In compositions of about 50%. Unfortunately, there is a transition from direct to indirect gap³⁸ when the Al content is higher than 25%. Without the identification of the different states at the $k=(0,0,0)$ point, it was not possible to obtain a good description of the behavior of the band gap in the entire the composition range in this case.

IV. CONCLUSIONS

Summarizing, the standard GQCA method used successfully in previous studies of nitride-based ternary alloys was extended to the quaternary alloys of the kind $A_xB_yC_{1-x-y}D$ (or $A_xB_yC_{1-x-y}$). By combining first-principles total energy calculations and the cluster expansion method within the framework of the GQCA approach, we made theoretical investigations of structural and electronic properties of unstrained $\text{Al}_x\text{Ga}_y\text{In}_{1-x-y}\text{X}$ ($\text{X}=\text{N}, \text{P}, \text{or As}$) quaternary alloys in the zinc-blende structure. Results for the bond lengths showed that the variation with composition is approximately linear and also does not deviate much from the values of the binary compounds. The maximum variation observed was 3.6% for the In-N bond length. In the case of AlGaInN, for the composition variation of the band gap, and its comparison to the experimental data for the wurtzite phase, we obtained a good agreement despite the evidence for cluster formation in these alloys. A bowing parameter of 0.22 eV was obtained for zinc-blende AlGaInN lattice matched with GaN. Finally, we obtained a bowing parameter $b=0.26$ eV for $(\text{Ga}_{0.47}\text{In}_{0.53}\text{As})_z(\text{Al}_{0.48}\text{In}_{0.52}\text{As})_{1-z}$ lattice matched with InP, in very good agreement with experimental data.

ACKNOWLEDGMENTS

We acknowledge support from the Science Funding Agency of the State of São Paulo (FAPESP), the Brazilian National Research Council (CNPq) through Grant No. 550.015/01-09/NanoSemiMat, and the Deutsche Forschungsgemeinschaft (Grant No. Be 1346/18-1).

- ¹J. Li, K. B. Nam, K. H. Kim, J. Y. Lin, and H. X. Jiang, *Appl. Phys. Lett.* **78**, 61 (2001).
- ²V. Adivarahan, A. Chitnis, J. P. Zhang, M. Shatalov, J. W. Yang, G. Simin, M. Asif Khan, R. Gaska, and M. S. Shur, *Appl. Phys. Lett.* **79**, 4240 (2001).
- ³A. Yasan, R. McClintock, K. Mayes, S. R. Darvish, P. Kung, and M. Razegui, *Appl. Phys. Lett.* **81**, 801 (2002).
- ⁴S. Nagahama, T. Yanamoto, M. Sano, and T. Mukai, *Jpn. J. Appl. Phys., Part 1* **40**, L788 (2001).
- ⁵T. Fujii, Y. Nakata, Y. Sigiya, and S. Hiyamizu, *Jpn. J. Appl. Phys.* **25**, L254 (1986).

- ⁶D. Olego, T. Y. Chang, E. Silberg, E. A. Caridi, and A. Pinczuk, *Appl. Phys. Lett.* **41**, 476 (1982).
- ⁷H. Hirayama, A. Kinoshita, T. Yamabi, Y. Enomoto, A. Hirata, T. Araki, Y. Nanishi, and Y. Aoyagi, *Appl. Phys. Lett.* **80**, 207 (2002).
- ⁸T. Takayama, M. Yuri, K. Itoh, T. Baba, and J. S. Harris, Jr., *J. Cryst. Growth* **222**, 29 (2001).
- ⁹A. Koukitsu, Y. Kumegai, and H. Seki, *J. Cryst. Growth* **221**, 743 (2000).
- ¹⁰S.-W. Feng, Y.-C. Cheng, Y.-Y. Chung, C. C. Yang, K.-J. Ma, C.-C. Yan, C. Hsu, J. Y. Lin, and H. X. Jiang, *Appl. Phys. Lett.*

- 82**, 1377 (2003).
- ¹¹C. H. Chen, Y. F. Chen, Z. H. Lan, L. C. Chen, K. H. Chen, H. X. Jiang, and J. Y. Lin, *Appl. Phys. Lett.* **84**, 1480 (2004).
 - ¹²M. Marques, L. K. Teles, L. M. R. Scolfaro, L. G. Ferreira, and J. R. Leite, *Phys. Rev. B* **70**, 073202 (2004).
 - ¹³M. Marques, L. G. Ferreira, L. K. Teles, and L. M. R. Scolfaro, *Phys. Rev. B* **71**, 205204 (2005).
 - ¹⁴L. K. Teles, J. Furthmüller, L. M. R. Scolfaro, J. R. Leite, and F. Bechstedt, *Phys. Rev. B* **62**, 2475 (2000).
 - ¹⁵L. K. Teles, L. M. R. Scolfaro, J. R. Leite, J. Furthmüller, and F. Bechstedt, *J. Appl. Phys.* **92**, 7109 (2002).
 - ¹⁶L. K. Teles, J. Furthmüller, L. M. R. Scolfaro, J. R. Leite, and F. Bechstedt, *Phys. Rev. B* **63**, 085204 (2001).
 - ¹⁷L. K. Teles, L. M. R. Scolfaro, J. R. Leite, J. Furthmüller, and F. Bechstedt, *Appl. Phys. Lett.* **80**, 1177 (2002).
 - ¹⁸A. Tabata, L. K. Teles, L. M. R. Scolfaro, J. R. Leite, A. Kharchenko, T. Frey, D. J. As, D. Schikora, K. Lischka, J. Furthmüller, and F. Bechstedt, *Appl. Phys. Lett.* **80**, 769 (2002).
 - ¹⁹J. W. D. Connolly and A. R. Williams, *Phys. Rev. B* **27**, 5169 (1983).
 - ²⁰A.-B. Chen and A. Sher, *Semiconductor Alloys* (Plenum Press, New York, 1995).
 - ²¹G. Kresse and J. Furthmüller, *Comput. Mater. Sci.* **6**, 15 (1996); *Phys. Rev. B* **54**, 11169 (1996).
 - ²²P. Hohenberg and W. Kohn, *Phys. Rev.* **136**, B864 (1964); W. Kohn and L. J. Sham, *Phys. Rev.* **140**, A1133 (1965).
 - ²³D. Vanderbilt, *Phys. Rev. B* **41**, 7892 (1990).
 - ²⁴J. P. Perdew and A. Zunger, *Phys. Rev. B* **23**, 5048 (1981).
 - ²⁵H. J. Monkhorst and J. D. Pack, *Phys. Rev. B* **13**, 5188 (1976).
 - ²⁶M. Marques, L. K. Teles, L. M. R. Scolfaro, J. R. Leite, J. Furthmüller, and F. Bechstedt, *Appl. Phys. Lett.* **83**, 890 (2003).
 - ²⁷N. J. Jeffs, A. V. Blant, T. S. Cheng, C. T. Foxon, C. Bailey, P. G. Harrison, J. F. W. Mosselmann, and A. J. Dent, *Mater. Res. Soc. Symp. Proc.* **512**, 519 (1998).
 - ²⁸K. E. Miyano, J. C. Woicik, L. H. Robins, C. E. Bouldin, and D. K. Wickenden, *Appl. Phys. Lett.* **70**, 2108 (1997).
 - ²⁹T. Saito and Y. Arakawa, *Phys. Rev. B* **60**, 1701 (1999).
 - ³⁰S. M. Sze, *Physics of Semiconductor Devices* (Wiley, New York, 1981).
 - ³¹S.-G. Chen and X.-Q. Fan, *J. Phys.: Condens. Matter* **9**, 3151 (1997).
 - ³²F. Sökeland, M. Rohlfing, P. Krüger, and J. Pollmann, *Phys. Rev. B* **68**, 075203 (2003).
 - ³³J. Schörmann, S. Potthast, M. Schnietz, S. F. Li, D. J. As, and K. Lischka, *Phys. Status Solidi C* (to be published).
 - ³⁴V. Yu. Davydov, A. A. Klochikhin, R. P. Seisyan, V. V. Emtsev, S. V. Ivanov, F. Bechstedt, J. Furthmüller, H. Harima, A. V. Mudryi, J. Aderhold, O. Semchinova, and J. Graul, *Phys. Status Solidi B* **229**, R1 (2002).
 - ³⁵V. Yu. Davydov, A. A. Klochikhin, V. V. Emtsev, D. A. Kurdyukov, S. V. Ivanov, V. A. Vekshin, F. Bechstedt, J. Furthmüller, J. Aderhold, J. Graul, A. V. Mudryi, H. Harima, A. Hashimoto, A. Yamamoto, and E. E. Haller, *Phys. Status Solidi B* **234**, 787 (2002).
 - ³⁶F. Bechstedt, J. Furthmüller, M. Ferhat, L. K. Teles, L. M. R. Scolfaro, J. R. Leite, V. Yu. Davydov, O. Ambacher, R. Goldhahn, *Phys. Status Solidi A* **195**, 628 (2003).
 - ³⁷*Gallium Nitride (GaN) I and II, Semiconductors and Semimetals*, edited by J. I. Pankove and T. D. Moustakas, Vol. 50 (Academic Press, New York, 1998); *ibid.* Vol. 57 (Academic Press, New York, 1999).
 - ³⁸S. P. Nadja, A. H. Kean, M. D. Dawson, and G. Duggan, *J. Appl. Phys.* **77**, 3412 (1995).
 - ³⁹F. G. McIntosh, K. S. Boutros, J. C. Roberts, S. M. Bedair, E. L. Piner, and N. A. el-Masry, *Appl. Phys. Lett.* **68**, 40 (1996).
 - ⁴⁰M.-Y. Ryu, C. Q. Chen, E. Kuokstis, J. W. Yang, G. Simin, M. A. Khan, and S. P. w. Yu, *Appl. Phys. Lett.* **80**, 3943 (2002).
 - ⁴¹S. Yamaguchi, M. Kariya, S. Nitta, H. Kato, T. Takeuchi, C. Wetzel, H. Amano, and I. Akasaki, *J. Cryst. Growth* **195**, 309 (1998).
 - ⁴²J. I. Davies, A. C. Marshall, M. D. Scott, and R. J. M. Griffiths, *Appl. Phys. Lett.* **53**, 276 (1988).
 - ⁴³R. F. Kopf, H. P. Wei, A. P. Perley, and G. Livescu, *Appl. Phys. Lett.* **60**, 2386 (1992).
 - ⁴⁴L. A. Cury, J. Beerens, and J. P. Praseuth, *Appl. Phys. Lett.* **63**, 1804 (1993).
 - ⁴⁵J. Böhler, A. Krost, and D. B. Bimberg, *Appl. Phys. Lett.* **63**, 1918 (1993).
 - ⁴⁶J. C. Fan and Y. F. Chen, *J. Appl. Phys.* **80**, 1239 (1996).
 - ⁴⁷I. Vurgaftman, J. R. Meyer, and L. R. Ram-Mohan, *J. Appl. Phys.* **89**, 5815 (2001).
 - ⁴⁸J. Han, J. J. Figiel, G. A. Petersen, S. M. Myers, M. H. Crawford, and M. A. Banas, *Jpn. J. Appl. Phys., Part 1* **39**, 2372 (2000).
 - ⁴⁹M. E. Aumer, S. F. LeBoeuf, F. G. McIntosh, and S. M. Bedair, *Appl. Phys. Lett.* **75**, 3315 (1999).